

A study of quantum well solar cell structures with bound-to-continuum transitions for reduced carrier recombination

G. Jolley, L. Faraone, L. Fu, H. F. Lu, H. H. Tan et al.

Citation: *Appl. Phys. Lett.* **102**, 213903 (2013); doi: 10.1063/1.4807506

View online: <http://dx.doi.org/10.1063/1.4807506>

View Table of Contents: <http://apl.aip.org/resource/1/APPLAB/v102/i21>

Published by the [AIP Publishing LLC](#).

Additional information on *Appl. Phys. Lett.*

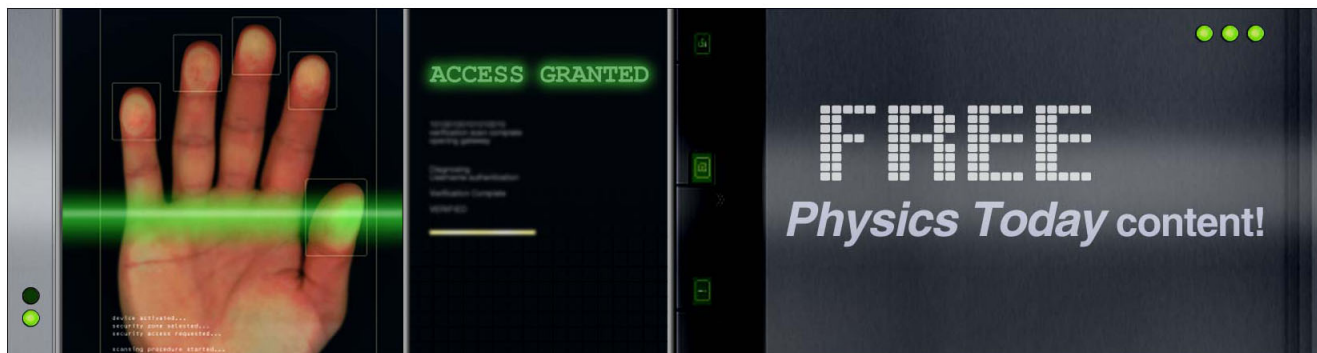
Journal Homepage: <http://apl.aip.org/>

Journal Information: http://apl.aip.org/about/about_the_journal

Top downloads: http://apl.aip.org/features/most_downloaded

Information for Authors: <http://apl.aip.org/authors>

ADVERTISEMENT



A study of quantum well solar cell structures with bound-to-continuum transitions for reduced carrier recombination

G. Jolley,^{1,a)} L. Faraone,¹ L. Fu,² H. F. Lu,² H. H. Tan,² and C. Jagadish²

¹School of Electrical, Electronic and Computer Engineering, The University of Western Australia, Crawley, WA 6009, Australia

²Department of Electronic Materials Engineering, Research School of Physics and Engineering, The Australian National University, Canberra, ACT 0200, Australia

(Received 9 April 2013; accepted 6 May 2013; published online 29 May 2013)

A bound-to-continuum quantum well solar cell structure is proposed, and the band structure and absorption spectra are analyzed by the use of an eight band $\mathbf{k} \cdot \mathbf{p}$ model. The structure is based on quantum wells that only support bound states for the valence band. The absence of bound conduction band states has a number of potential advantages, including a reduction of electron trapping and, therefore, a reduction of quantum well induced photocarrier recombination due to reduced spatial overlap of the electron and hole wavefunctions. © 2013 AIP Publishing LLC. [<http://dx.doi.org/10.1063/1.4807506>]

In comparison with single junction solar cells constructed from only the wider band gap barrier material, quantum well solar cells (QWSCs) have the advantage of extending the spectral response to longer wavelengths, thus leading to an increase of the photocurrent.^{1,2} QWSCs typically have a p-i-n configuration with the quantum wells (QWs) embedded within the depleted intrinsic region, thus minimizing the steady-state charge carrier occupation of the QWs and preventing excessive QW induced carrier recombination. The total built-in electric field across the p-i-n junction is determined by the Fermi-level locations of the doped base and emitter layers, which are constructed from the wider band gap barrier material. Consequently, it is possible to independently optimize both the open-circuit voltage (V_{oc}) and short-circuit current (I_{sc}) of a QWSC which can lead to efficiencies beyond the single junction limit.³⁻⁶ However, it is generally observed experimentally that the incorporation of the narrower band gap QWs leads to a reduction of the V_{oc} due to QW induced enhancement of carrier recombination.⁷⁻⁹ QWSCs that consist of a variety of materials and band gaps have been studied extensively, and it has been reported that the addition of narrower band gap QWs increases the power conversion efficiency in comparison to single junction cells that are constructed from only the QW barrier material.⁹ However, all such measurements have been performed using a light source with an equivalent temperature that is far from optimum for the semiconductor band gap being used. Therefore, there are no reports of QWSCs with an improved efficiency in comparison to a single junction cell with a band gap that is optimally matched to the spectrum of light used in the reported measurements. In other words no QWSC has been observed to exceed the Shockley-Queisser efficiency limit. Apart from efforts to break the Shockley-Queisser efficiency limit, QWs have the potential to increase the efficiency of multi-junction cells by improved matching of the currents of the constituent cells. For example, InGaAs QWs incorporated in the GaAs bottom cell of an InGaP/GaAs tandem cell can significantly improve current matching and cell efficiency.^{10,11} Recently

In_{0.1}Ga_{0.9}As/GaAs_{0.93}P_{0.07} QWs have been included in an InGaP/GaAs tandem solar cell in an effort to increase efficiency.¹¹ Previous publications in this area have concluded that minimizing carrier recombination is a necessary requirement for the development of high efficiency multi-junction solar cells that incorporate QWs.

A range of material systems have been used in experimental studies of QWSCs, including GaAs/AlGaAs, InGaAs/GaAs, and InGaAs/InP. The most common and suitable material systems for the fabrication of III-V semiconductor QWSCs are type I heterojunctions, which tend to trap both electrons and holes and, thus, strongly influence carrier recombination. QWs that feature only bound-to-continuum (BC) transitions due to a lack of confined states for one type of carrier have been largely unexplored for solar cell applications. In this paper, we investigate a proposed QW structure that supports confined states for only the valence band and show that such a configuration can potentially result in a significant reduction in charge carrier recombination rates. A simplified band diagram of the proposed structure is shown in Fig. 1, as implemented in the InGaAs/AlGaAs/GaAs material system. The effects of QW strain and the large difference between the conduction band (CB) electron and valence band heavy hole (HH) effective masses both serve to suppress bound conduction band states. The hydrostatic strain of an InGaAs QW pseudomorphically strained to a GaAs substrate increases the confinement of heavy hole states whereas it reduces the binding energy of conduction band states. The

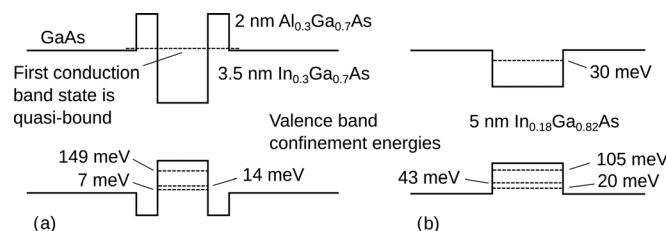


FIG. 1. (a) Band diagram of the bound-to-continuum InGaAs/AlGaAs/GaAs QWSC displaying the CB and VB confinement energies calculated for the structure parameters as shown. (b) Also included for comparison are the calculation results of a 5 nm thick In_{0.18}Ga_{0.82}As/GaAs QW.

^{a)}gregory.jolley@uwa.edu.au

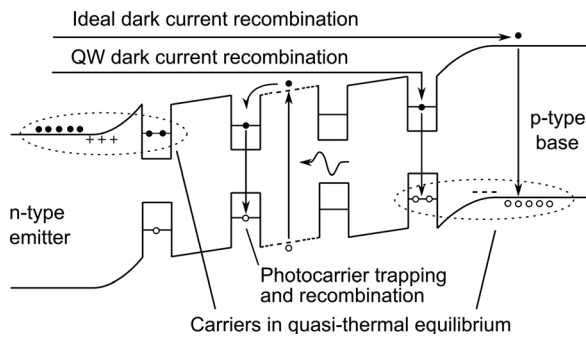


FIG. 2. Energy band diagram of a QWSC displaying the two mechanisms by which carriers can recombine, thus resulting in a reduction of the open-circuit voltage. Dark current carriers thermally injected from the emitter and base contact layers only have to overcome part of the depletion region potential to be captured by a QW near the opposite contact layer, which is heavily populated with charge carriers due to a modulation doping effect. This leads to a reduction of the dark current thermal activation energy. Also shown is the capture and recombination of photo-generated carriers by a QW.

incorporation of relatively thin InGaAs QWs will tend to result in a reduced confinement energy for carriers with a smaller effective mass. In addition, by including thin layers of wider bandgap AlGaAs, the conduction band QW states are pushed further into the GaAs barrier continuum level.

There are two principal mechanisms that degrade the V_{oc} of a QWSC: QW related recombination of photo-generated electron-hole pairs and an increase of the dark current due to a lowering of the dark current thermal activation energy. These two mechanisms are displayed in Fig. 2. Previous experimental studies of quantum dot and QW solar cells have indicated that the reduction of V_{oc} can be correlated directly with an increase in dark current,^{12–15} as shown schematically in Fig. 2. In most QWSCs at room temperature, photo-generated carrier escape processes proceed at a faster rate than competing recombination processes, and therefore it can be assumed that all photocarriers contribute to the photocurrent. Due to modulation doping effects, carriers will occupy the QW layers nearest to the doped base and emitter layers. Thus, thermally injected carriers originating from the base and emitter only travel through part of the depletion region before they recombine with the heavily populated QWs nearest to the doped contact layers. Note that the occupancy of the QW layers due to a modulation doping effect is not associated with a thermal activation energy. Therefore the thermal activation energy associated with dark current transport is predominantly due to the transport of carriers from a doped contact layer to a QW layer part way across the depletion region. The thermal activation energy associated with such a transport event is lower than the built-in potential, which leads to an increase in the dark current. Electroluminescence measurements have confirmed that dark current recombination in QWSCs occurs almost exclusively within the QWs, particularly for structures with 5 or more QWs.¹⁶ Solar cell dark current arises from non-equilibrium processes, and for a QWSC it is dependent on the rate of carrier injection into the depletion region and the probability that such carriers relax into QW confined states and recombine before being thermally emitted from the QW. Thus, eliminating confined CB states dramatically reduces the probability of thermally injected electrons being captured by the QWs, therefore

reducing the probability of recombination. Although injected holes have a high probability of being captured by the QWs, they are less likely to recombine if there are no trapped electrons occupying the QWs.

Other novel QWSC structures have been explored in an attempt to minimize photocarrier recombination and maximize the open-circuit voltage. Shiotsuka *et al.* reported on an experimental study of QWSCs based on QWs with a stepped potential profile.^{17,18} By employing a stepped profile it is suggested that faster QW carrier escape times can be achieved ideally leading to a reduction of carrier recombination. Welser *et al.* recently employed a similar scheme and compared the V_{oc} of stepped QWs with that of standard QWSCs, demonstrating an improved V_{oc} , albeit for a single stepped QW unit with a relatively wide QW bandgap of 1.32 eV.¹⁹ The central idea of a stepped QWSC is to engineer QWs with a number of closely spaced energy levels (≈ 35 meV) such that carriers are rapidly excited to higher energy levels by thermal excitation, resulting in an enhanced thermionic emission rate from the QWs in comparison to a regular QW structure. A careful consideration of the band structure of stepped potential profile QWs and the effect on carrier emission rates is required, since a greater density of closely spaced QW sub-band levels also implies efficient carrier relaxation. The BC structure presented in this paper supports no confined CB states so the effective escape time of electrons is the tunneling rate through the double barrier QW structure.

The absorption spectrum of the proposed QW structure shown in Fig. 1 has been calculated using an 8-band $\mathbf{k} \cdot \mathbf{p}$ model²⁰ with material parameters from Vurgaftman *et al.*,²¹ without including excitonic effects. The normal incidence absorption strength for a single quantum well layer is shown in Fig. 3. The BC requirements and QW growth limitations due to strain accumulation place restrictions upon the maximum width and In content of the InGaAs QW. Calculations indicate that the BC structure can achieve an absorption strength and bandgap energy similar to that of a 5 nm $\text{In}_{0.18}\text{Ga}_{0.82}\text{As}/\text{GaAs}$ QW, which has an absorption

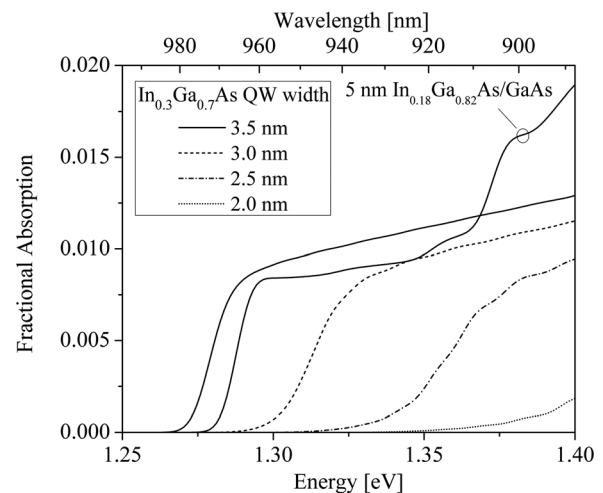


FIG. 3. Calculated absorption spectrum for the QW structure displayed in Fig. 1 for various thicknesses of the $\text{In}_{0.3}\text{Ga}_{0.7}\text{As}$ QW layer. The absorption spectrum is calculated for light incident perpendicular to the plane of the QW and is given as the fraction of light absorbed by a single QW unit. For comparison, the calculated absorption spectrum of a 5 nm thick $\text{In}_{0.18}\text{Ga}_{0.82}\text{As}/\text{GaAs}$ QW is also shown.

edge at about 1.27 eV (975 nm). Although the unstrained bandgap difference of 420 meV between GaAs and $\text{In}_{0.3}\text{Ga}_{0.7}\text{As}$ falls mostly across the CB, 278 meV compared with 142 meV for the VB, the hydrostatic strain of -0.0218 for an $\text{In}_{0.3}\text{Ga}_{0.7}\text{As}$ QW grown on a (001) oriented GaAs substrate reduces the CB potential offset to 123 meV and increases the heavy hole band potential offset to 199 meV. Due to a large effective mass, the first heavy hole state of the BC QW tends to have an energy close to the heavy hole band potential. For a 3.5 nm well width the calculated HH binding energy is 149 meV.

The BC QW only supports one significant bound valence band state, and, therefore, the absorption spectrum for the energy region below the GaAs bandgap is dominated by transitions from this valence band to conduction band states with an energy greater than the GaAs band edge. The calculated conduction band confinement energy of 30 meV for the $\text{In}_{0.18}\text{Ga}_{0.82}\text{As}/\text{GaAs}$ QW is rather low when compared to an unstrained InAs/GaAs conduction band offset of 0.89 eV. In addition to strain and the small conduction band effective mass, the bowing parameter of -0.38 eV for the InAs/GaAs valence band offset²¹ results in higher computed conduction band energies for InGaAs/GaAs QWs. It should, however, be noted that there is significant uncertainty in the values for the GaAs/InAs valence band offset and its bowing parameter.²¹

Despite the absence of bound CB states, the BC QW can still achieve an absorption strength that is comparable to that of the 5 nm $\text{In}_{0.18}\text{Ga}_{0.82}\text{As}/\text{GaAs}$ QW. The effects of QW confinement on the absorption strength of the BC structure has been investigated by undertaking calculations for a variety of QW widths, the results of which are shown in Fig. 3. The QW width is found to influence both the rate at which the absorption strength increases with energy and the maximum obtained value. It is important to note that the BC QW exhibits absorption strengths similar to regular QWs because of the high degree of spatial overlap between the HH ground state and quasi-bound CB envelope wavefunctions. Within the eight-band $\mathbf{k} \cdot \mathbf{p}$ model, the optical absorption cross section between an initial VB state, $|i\rangle$, and a final CB state, $|f\rangle$, is given by

$$\sigma = \frac{2\pi}{nc\epsilon_0\omega m_0^2} |\langle i|\mathbf{p} \cdot \boldsymbol{\varepsilon}|f\rangle|^2 \delta(E_i - E_f - \hbar\omega), \quad (1)$$

where e is the charge of an electron, m_0 is the electron rest mass, ϵ_0 is the permittivity of free space, c is the speed of light in vacuum, n is the refractive index, and ω is the angular frequency of the transition. The momentum operator, \mathbf{p} , acts between the initial and final states and $\boldsymbol{\varepsilon}$ is the polarization vector of the absorbed light. For these calculations it is assumed that light is incident perpendicular to the plane of the QW. Expanding out the action of the momentum operator and noting that $\langle u_n|u_{n'}\rangle \approx \delta_{n,n'}$,

$$\left| \left\langle \sum_{n=1}^8 u_n \psi_{i,n} | \mathbf{p} \cdot \boldsymbol{\varepsilon} | \sum_{n'=1}^8 u_{n'} \psi_{f,n'} \right\rangle \right|^2 \approx \left| \sum_{n=1}^8 \sum_{n'=1}^8 \langle \psi_{i,n} | \psi_{f,n'} \rangle \langle u_n | \mathbf{p} \cdot \boldsymbol{\varepsilon} | u_{n'} \rangle \right|^2, \quad (2)$$

where $|u_n\rangle$ is the eight Bloch basis functions and $|\psi_n\rangle$ is the corresponding envelope wavefunctions. Since the VB ground state subband predominantly has a HH character, the optical absorption cross section for transitions from the ground state subband is dependent on the following term:

$$|\langle u_{HH} | \mathbf{p} \cdot \boldsymbol{\varepsilon} | u_{CB} \rangle|^2 |\langle \psi_{HH} | \psi_{CB} \rangle|^2. \quad (3)$$

Since $|\langle u_{HH} | \mathbf{p} \cdot \boldsymbol{\varepsilon} | u_{CB} \rangle|$ remains constant, the absorption strength depends on the envelope wavefunction overlap term, $|\langle \psi_{HH} | \psi_{CB} \rangle|$. The CB envelope wavefunctions, $|\psi_{CB}\rangle$, are approximately complete and orthogonal. Therefore, the ground state HH envelope wavefunction can be expressed uniquely as a linear combination of the CB states

$$|\psi_{HH}\rangle = \sum_n a_n |\psi_{CB}^n\rangle, \quad (4)$$

where the a_n terms are weighting coefficients and ψ_{CB}^n correspond to all the CB states. Considering transitions from an initial VB state to all final CB states, the total sum absorption strength to all transitions is limited by the term

$$\sum_n |\langle \psi_{HH} | \psi_{CB}^n \rangle|^2 \approx 1. \quad (5)$$

If the quasi-bound CB states have a large wavefunction overlap with the HH ground state, then the CB states of higher energy will have a small overlap with the HH ground state wavefunction. Under such conditions the optical absorption near the QW band gap is high. The BC QW can have large absorption near the QW band gap because the potential of the InGaAs QW results in quasi-bound states with a large wavefunction component within the QW region. Although these quasi-bound states have an energy that is very close to the GaAs band edge, they have a large percentage of wavefunction that occupies the InGaAs QW. The energies at which the CB states become quasi-bound to the InGaAs QWs depend on the thickness of the InGaAs QW. For large InGaAs well widths the quasi-bound states have an energy close to the GaAs band edge, and as the thickness is reduced the quasi-bound states increase in energy. This is reflected in the absorption spectra of Figure 3.

In general, a single QW absorbs of the order of 1% of the light incident upon it, which dictates that stacks with a large number of QWs are required to obtain a high level of light absorption and, hence, quantum efficiency. The use of textured dielectric thin film techniques that result in incident light making multiple passes through the cell can be of particular benefit to QWSCs in order to obtain a larger I_{sc} . However, it should be noted that the full benefits that photon recycling can bring to minimizing solar cell dark current can only be obtained for a strong absorber.²²

The compressive strain in the InGaAs QWs can be balanced by the incorporation of a small amount of phosphorus in the GaAs barrier layers ($\text{GaAs}_{1-x}\text{P}_x$). However, the local InGaAs QW strain is high, and so this approach can compromise the material quality. In addition, the width of the QW band gap is limited to energies close to that of the GaAs barrier. Adding small amounts of Sb to the InGaAs QW could

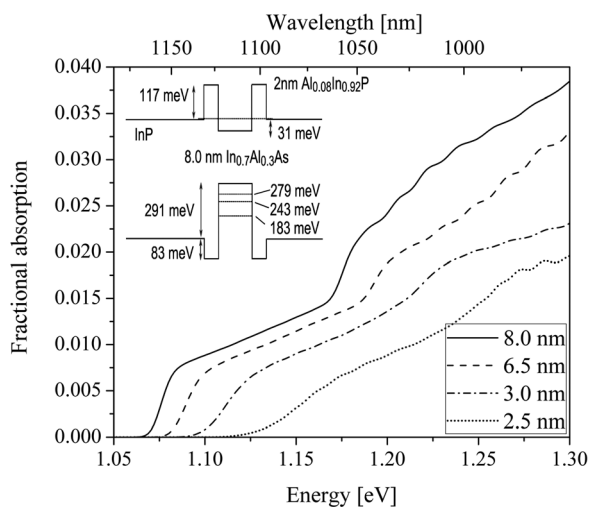


FIG. 4. Calculated absorption spectrum for the QW structure displayed in the inset figure for various thicknesses of the $\text{In}_{0.7}\text{Al}_{0.3}\text{As}$ QW layer. The inset figure displays the calculated confinement energy levels for an 8 nm thick $\text{In}_{0.7}\text{Al}_{0.3}\text{As}$ layer, and the strained conduction band and heavy hole band edge energies are listed.

be an ideal way of increasing the VB binding energy resulting in a narrower QW band gap. GaSb has a large VB offset potential, and GaAs/GaSb forms a type II hetero-junction with CB electrons confined to the GaAs layers. Therefore adding small amounts of Sb to the InGaAs QW will enhance the VB confinement potential while reducing the CB confinement potential. Unfortunately, GaAsSb/GaAs QWs are not suitable for BC structures because it is not possible to create quasi-confinement of CB wavefunctions in the GaAsSb QW, since its CB potential is greater than that of GaAs.

The InAlAs/InAlP/InP material system is also suitable for the fabrication of BC QWSCs. Calculations for a set of $\text{In}_{0.7}\text{Al}_{0.3}\text{As}/\text{Al}_{0.08}\text{In}_{0.92}\text{P}/\text{InP}$ QWs are shown in Fig. 4. Deeper VB confinement energies are possible for this material system since InP has a relatively large unstrained VB offset potential of -0.98 eV compared with GaAs, which is -0.8 eV . The relatively shallow conduction band confinement potential of the strained $\text{In}_{0.7}\text{Al}_{0.3}\text{As}$ layer allows it to be significantly thicker while maintaining no bound conduction band states. Calculations indicate that 8 nm is the upper thickness limit of this layer in order to ensure that there are no bound states. Since the QW is relatively thick and the VB potential offset is larger, a number of bound VB states are supported, the first three of which are shown in Fig. 4. The first two subbands with binding energies of 279 meV and 243 meV are heavy hole subbands, and the one at 183 meV is a light-hole subband. The second heavy hole subband to quasi-bound CB absorption is evidently weak, which is due to differences in the symmetries of the envelope wavefunctions of these subbands. In general, the absorption strength of the BC structures can be very similar to regular type-I QWs provided the QW width and potential are designed such that the QW CB states are quasi-bound with an energy close to the GaAs barrier band-edge.

Although the BC QW can exhibit an absorption strength similar to a regular QW without the trapping of electrons, the ultimate performance limitations of a solar cell incorporating

this type of QW is dependent on a number of complicated and inter-related factors. For a given QW band gap, holes in a BC QW will have a greater binding energy than a regular QW. Therefore longer thermal emission time constants can be expected for holes. Also, holes occupy those QWs nearest the p-doped base layer, which influences the electric field throughout the structure which, in-turn, affects the transportation of dark current electrons.

In summary, QWSC structures with QWs that support only bound valence band states have been proposed as an alternative to standard QWs due to the potential benefit of reduced carrier recombination as a consequence of suppression of electron trapping. Calculations indicate that the absorption strength of the bound-to-continuum transitions of these structures is very similar to regular QWs. Strong absorption results from the quasi-bound nature of the conduction band states, which is a consequence of the attractive potential of the QW.

Thanks are due to the Australian Research Council for the financial support of this research.

- ¹P. Kailuweit, R. Kellenbenz, S. P. Philipps, W. Guter, A. W. Bett, and F. Dimroth, *J. Appl. Phys.* **107**, 064317 (2010).
- ²M. Paxman, J. Nelson, B. Braun, J. Connolly, K. W. J. Barnham, C. T. Foxon, and J. S. Roberts, *J. Appl. Phys.* **74**, 614 (1993).
- ³K. W. J. Barnham and G. Duggan, *J. Appl. Phys.* **67**, 3490–3493 (1990).
- ⁴K. W. J. Barnham, B. Braun, J. Nelson, M. Paxman, C. Button, J. S. Roberts, and C. T. Foxon, *Appl. Phys. Lett.* **59**, 135 (1991).
- ⁵N. G. Anderson, *J. Appl. Phys.* **78**, 1850–1861 (1995).
- ⁶S. P. Bremner, R. Corkish, and C. B. Honsberg, *IEEE Trans. Electron. Devices* **46**, 1932–1939 (1999).
- ⁷N. G. Anderson and S. J. Wojtczuk, *J. Appl. Phys.* **79**, 1973–1978 (1996).
- ⁸N. J. Ekins-Daukes, K. W. J. Barnham, J. P. Connolly, J. S. Roberts, J. C. Clark, G. Hill, and M. Mazzer, *Appl. Phys. Lett.* **75**, 4195 (1999).
- ⁹K. Barnham, J. Connolly, P. Griffin, G. Haarpaintner, J. Nelson, E. Tsui, A. Zachariou, J. Osborne, C. Button, G. Hill, M. Hopkinson, M. Pate, and J. Roberts, *J. Appl. Phys.* **80**, 1201–1206 (1996).
- ¹⁰N. J. Ekins-Daukes, J. Barnes, K. W. J. Barnham, J. P. Connolly, M. Mazzer, J. C. Clark, R. Grey, G. Hill, M. Pate, and J. S. Roberts, *Sol. Energy Mater. Sol. Cells* **68**, 71–87 (2001).
- ¹¹J. G. J. Adams, B. C. Browne, I. M. Ballard, J. P. Connolly, N. L. A. Chan, A. Ioannides, W. Elder, P. N. Stavrinou, K. W. J. Barnham, and N. J. Ekins-Daukes, *Prog. Photovoltaics* **19**, 865–877 (2011).
- ¹²S. C. McFarlane, J. Barnes, K. W. J. Barnham, E. S. M. Tsui, C. Button, and J. S. Roberts, *J. Appl. Phys.* **86**, 5109–5115 (1999).
- ¹³I. Serdiukova, C. Monier, M. Vilela, and A. Freundlich, *Appl. Phys. Lett.* **74**, 2812 (1999).
- ¹⁴J. Barnes, J. Nelson, K. W. J. Barnham, J. S. Roberts, M. A. Pate, R. Grey, S. S. Dosanjh, M. Mazzer, and F. Ghirardo, *J. Appl. Phys.* **79**, 7775–7779 (1996).
- ¹⁵T. Tibbits, I. M. Ballard, K. W. J. Barnham, R. Day, C. Lim, M. Lynch, M. Mazzer, J. S. Roberts, and R. Airey, in *Proceedings of the 31st IEEE Photovoltaic Specialists Conference*, 2005, pp. 587–590.
- ¹⁶A. Bessière, J. P. Connolly, K. W. J. Barnham, M. F. Führer, M. Lynch, I. M. Ballard, M. Mazzer, D. C. Johnson, G. Hill, and J. S. Roberts, *J. Appl. Phys.* **107**, 44502–44505 (2010).
- ¹⁷N. Shiotsuka, T. Takeda, and Y. Okada, in *3rd World Conference on Photovoltaic Energy Conversion*, 2003, pp. 2750–2753.
- ¹⁸Y. Okada and N. Shiotsuka, in *Proceedings of Photovoltaic Specialists Conference*, 2005, pp. 591–594.
- ¹⁹R. E. Welser, *Proc. SPIE* **8256**, 82560C (2012).
- ²⁰T. B. Bahder, *Phys. Rev. B* **41**, 11992–12001 (1990).
- ²¹I. Vurgaftman, J. R. Meyer, and L. R. Ram-Mohan, *J. Appl. Phys.* **89**, 5815–5875 (2001).
- ²²D. C. Johnson, I. M. Ballard, K. W. J. Barnham, J. P. Connolly, M. Mazzer, A. Bessière, C. Calder, G. Hill, and J. S. Roberts, *Appl. Phys. Lett.* **90**, 213505 (2007).